

OBSERVATIONAL PROPERTIES OF COSMIC GAMMA-RAY BURSTS

E.P.Mazets

A.F.Ioffe Physical-Technical Institute,
Academy of Sciences of the USSR,
194021 Leningrad, USSR

1. Introduction. Intense impulsive fluxes of hard photons with an energy of ~ 1 keV to few tens of MeV propagate in interstellar space in our Galaxy. When such a very thin front of high photon density passes across the Solar System and meets a spacecraft with a gamma-ray detector aboard, the observer perceives what we call a gamma-ray burst. The pioneering observations of the gamma-ray bursts in the early '70s [1] were followed by their comprehensive investigation aimed at finding answers to the questions of where these very strong radiation fluxes come from, where and how they are produced. Despite the fact that much has been learned in the recent years, we still do not have full understanding of the origin of the bursts.

In their studies of the gamma-ray bursts, the astrophysicists have met with problems which are not only very intriguing but extremely complex as well.

The present paper is a brief overview of the major observational results obtained in gamma-ray burst studies. We will also discuss to what extent the thermonuclear model which appears at present to be the most plausible can account for the observed properties of the bursts. The investigation of gamma-ray bursts should cover observations of the time histories of events, of the energy spectra and of their variability, source localization and inspection of the localization regions during the active and quiescent phases of the source in other wavelengths as well as evaluation of the statistical distributions of the data obtained.

2. Time Structure of the Gamma-Ray Bursts. The bursts vary in duration over a wide range from around ten milliseconds to a few minutes. The time histories of the bursts are extremely diverse. Several attempts have been made at constructing a morphological classification of the events [2,3]. Subsequent observations confirm the existence of several types of time structures. Fig.1 shows several light curves measured in the Konus experiment on Venera 13 and 14 in the energy range 45-200 keV. Note that because of the spectral variability of radiation the time profiles observed in different energy intervals may differ slightly.

First one should point out the existence of two classes of events. Short bursts (GB811220, Fig.1), apart from their short duration, $< 0.5-1$ s, differ strongly from long events in the short rise time, $\sim 10-100$ ms [4-6]. Among long bursts one may discriminate at least two groups of events.

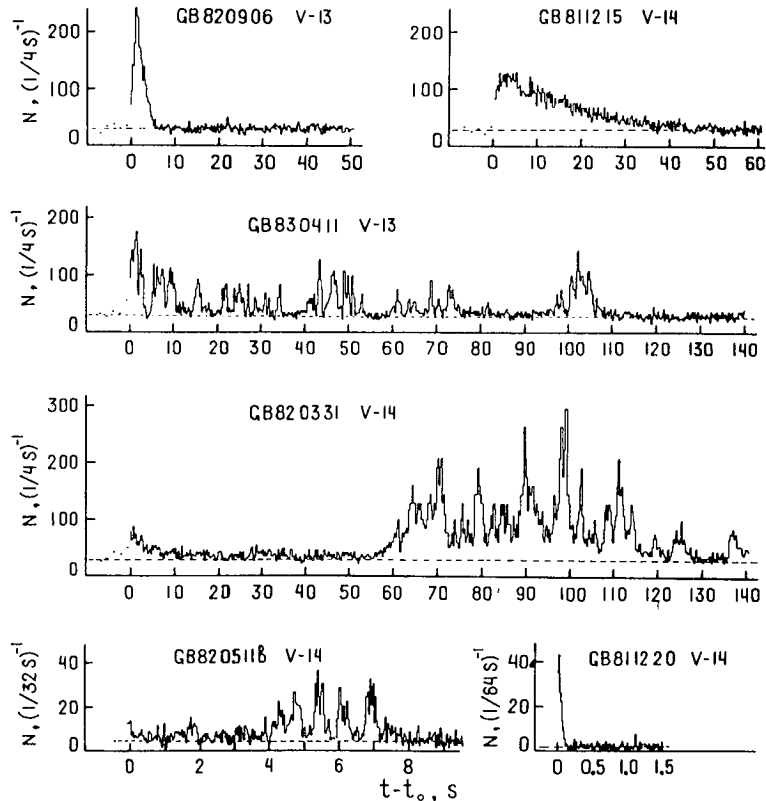


Fig.1. Typical time histories of gamma-ray bursts

Simple single-pulse bursts (GB820906) last for 5-15 s. In some cases their duration increases by a few times making them look like long structureless events (GB811215). The most numerous are bursts with a complex multipulse time structure. The number of individual peaks observed in the profile may vary reaching sometimes a few tens (GB830411). Quite frequently these peaks may form quasiperiodic trains. However barring a few exclusions, no strictly regular periodicity is observed in the burst profiles [7,8]. As a rule, the rise and decay times of individual peaks in complex bursts are shorter than those in single-pulse events. It appears that many bursts reveal a peculiar trend in their time structure. If a burst develops faster, i.e. a burst with a complex structure is shorter, then the details in its time structure are compressed accordingly (GB820511). This remarkable feature of a similarity between the time histories of various bursts analyzed on a normalized, compressed or extended, time scale was pointed out in several observations [9,10]. In many cases one observes in the pro-

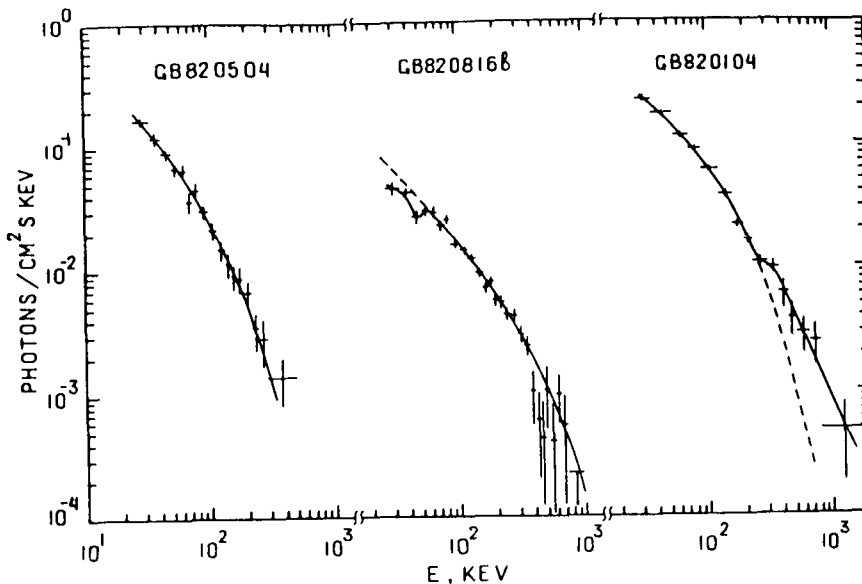


Fig.2. Typical burst energy spectra: typical continuum, spectrum with a cyclotron feature, spectrum with an annihilation feature

files precursors preceding by a few tens of seconds the main phase of the burst (GB820331). The observation of weak precursors is apparently limited by the instrument sensitivity. If the precursors are indeed a widespread feature of the bursts, then their observations should become more numerous as the sensitivity of gamma-ray burst detectors increases. The time structures of the bursts reflect obviously the inherent and most essential characteristics of the emission processes in the sources. Explanation of the time evolution of the bursts should be a major goal in the construction of any source model. Unfortunately, most of the models being developed at present focus on the energetics of the sources and on the energy spectra while paying little attention to the time structures.

3. Energy Spectra. In contrast to the time structure, the energy spectra of the bursts display a markedly uniform pattern [11]. With the present-day measurement accuracy, the smooth continua observed in the energy range 30 keV - 2 MeV (see, e.g. the spectrum of the 4 May 1982 event, Fig.2) may be fitted equally well by optically thin thermal bremsstrahlung or thermal synchrotron distributions [12,13]. The actual mechanism of emission still remains unclear [14-17]. Assuming the emission to be of thermal nature, estimates of the temperature in the sources range from 10^9 to 10^{10} K. In many cases the energy spectra were found

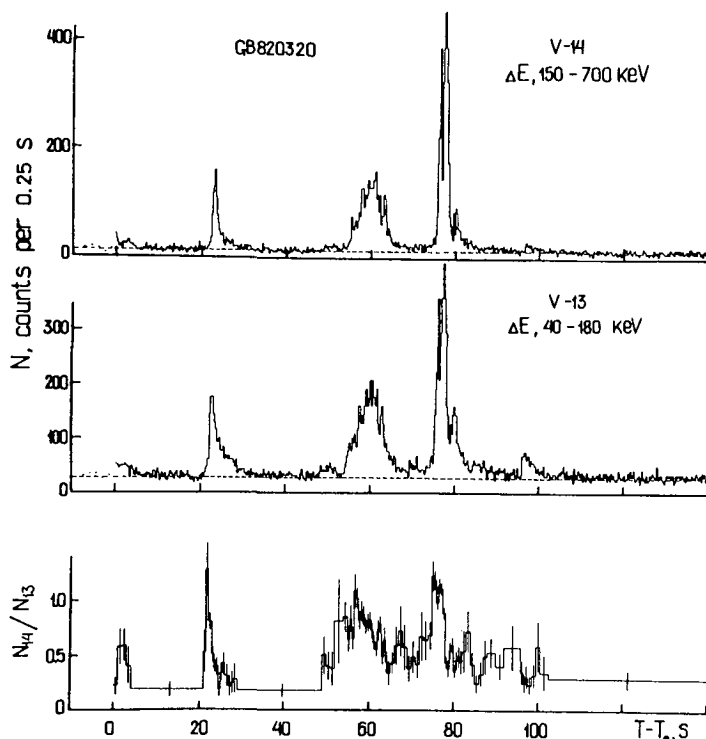


Fig.3. Gamma-ray burst time profiles in the various energy ranges. The hardness ratio indicates a fast and strong spectral variability

to reveal spectral features of two types [18]. The absorption features are observed in the energy range 30 - 100 keV (GB820816, Fig.2). They are believed to originate from cyclotron absorption at magnetic fields

$B \sim (2-8) \times 10^{12}$ G. The emission features peak in the range 350-450 keV (GB820104, Fig.2). These features are most probably due to gravitationally redshifted pair annihilation emission.

This interpretation has led to the

presently widely accepted opinion that cosmic gamma-ray bursts are generated by strongly magnetized neutron stars.

The energy spectra are characterized by a strong and fast spectral variability [11,19,20]. The continua measured in different phases of a burst differ essentially, as a rule, in accordance with temperature variations of the emitting region. Spectral hardness may vary as fast as the emission intensity does. Fig.3 displays time profiles of GB820320 obtained in various energy intervals as well as the corresponding variations of the hardness ratio.

Spectral features also evolve rapidly. The cyclotron features are observed primarily in the initial stages of the bursts. The annihilation radiation is likewise the strongest in the beginning of a burst or is connected with the most intense peaks in the time structure.

In the recent two-three years new essential information on the burst spectra has been obtained. SMM observations have revealed a high energy component in the burst spectra (Fig.4) [21,22]. By our data, the hard tails in the

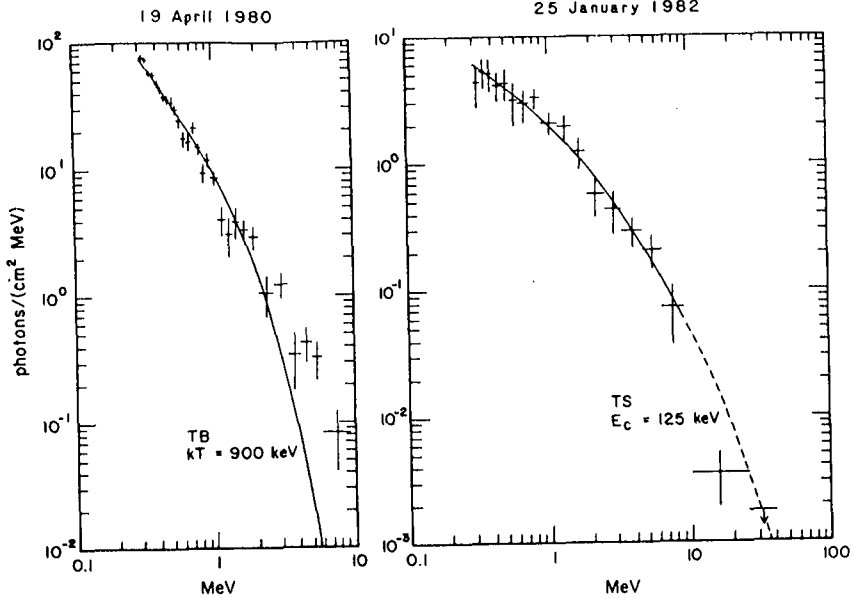


Fig.4. High energy emission in gamma-ray bursts from SMM data [22].

spectra are directly associated with the annihilation features and represent actually their extension. An investigation of a large number of spectra containing emission features has shown the spectral distribution of the annihilation radiation to be a broad line with an extended hard wing (Fig.5). This implies that the energy spectra of bursts consist of two emission components. Their angular patterns are assumed to be different [23].

The spectral shape of the softer continuum emission is affected by the absorption of hard photons involving pair formation. The angular distribution of this emission is close to isotropic.

The observed annihilation spectrum is apparently produced by superposition of in-

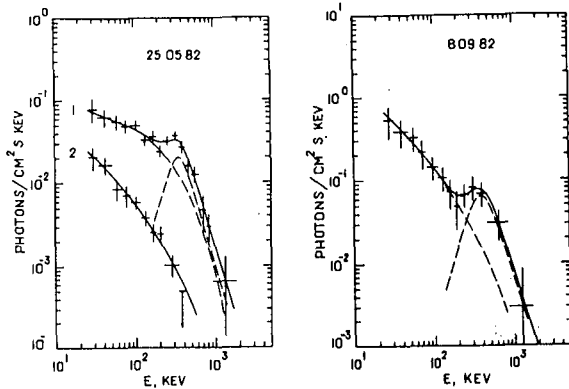


Fig.5. Two emission components in gamma-ray burst spectra. (a) Time evolution of a spectrum with annihilation feature. (b) Annihilation feature in a spectrum of a short burst of 100 ms duration.

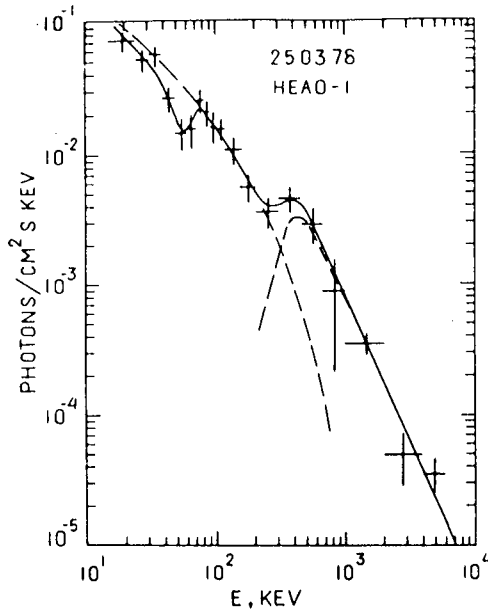


Fig.6. HEAO-1 observations of a complex spectrum [26]

observations in an X-ray range 3-10 keV [27] (Fig.7). As shown by these observations, the X-ray luminosity of the burst sources is high, $L_X/L_\gamma \sim 0.02$, the X-ray emission is somewhat delayed compared with the time profile in gamma rays. The X-ray tail following the main phase may indicate cooling of the emitting region.

4. Optical Flashes.

Operation of an international network of satellite-borne gamma-ray burst detectors has resulted in a remarkable achievement, namely, an exact localization on the celestial sphere of a number of burst sources with an error box size of $\lesssim 1$ arc minute [28, 29]. It was found that these error boxes do not contain easily

stantaneous annihilation spectra [24] generated by a pair-dominated plasma with a fast and strongly varying temperature. It is also possible that this spectrum is directly related with the close-to-power law energy distribution of electrons and positrons [25] in their one-dimensional motion along the magnetic field lines. The radiation is emitted most probably from the polar region of a neutron star in a collimated beam.

A remarkable illustration of a spectrum with both a cyclotron absorption line and an intense annihilation component is provided by HEAO-1 observations of GB780325 [26] (Fig.6).

Quite recently very interesting results have been obtained in gamma-ray burst

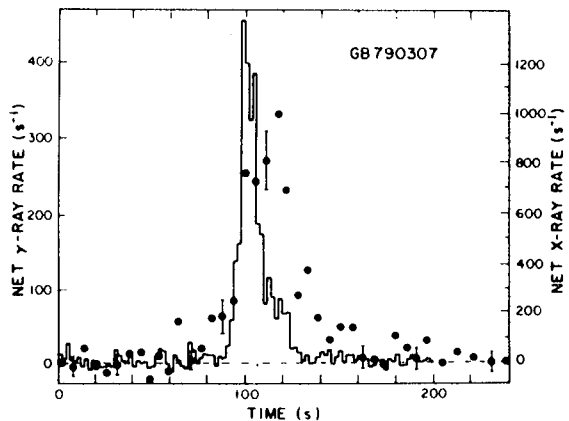


Fig.7. Simultaneous burst observations in gamma- and X-rays [27]

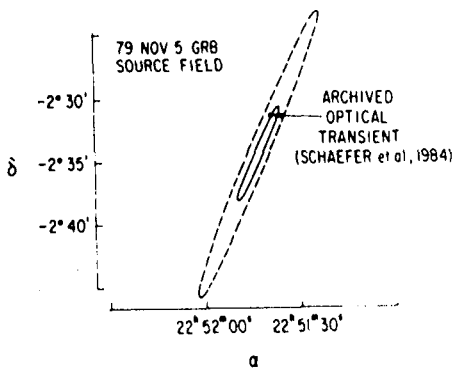


Fig.8. Error box of the 5 November 1979 event. Position of the optical flash on an archival photographic plate of 1941 [29]

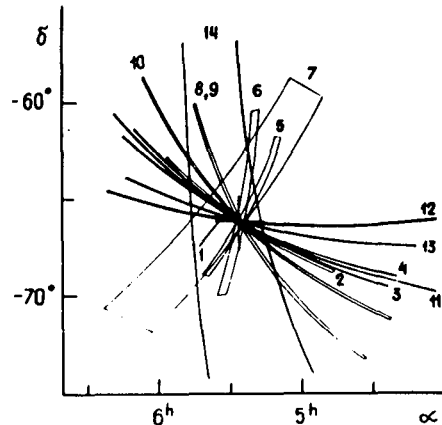


Fig.9. Error boxes for a series of recurrent bursts from GBS0526-66

detectable radio, optical or X-ray objects. Only a deep search carried out at a very high sensitivity reveals in these regions a few weak objects. It would be very difficult to identify any of these objects as the optical counterparts of the burst sources in quiescent state [29].

All the more unexpected was the discovery on archival photographic plates of optical flashes in the error boxes of three gamma-ray burst sources [30,31] (Fig.8). The reliability of identification of these flashes with gamma-ray burst sources is apparently no more questioned at present. The ratio of the energy in the optical flash to that of the gamma-ray burst observed many years thereafter is

$E_{\text{opt}}/E_{\gamma} \sim 10^{-3}$. The discovery of optical flashes will undoubtedly produce a strong impact on possible models of gamma-ray bursts.

The most remarkable feature of the famous source of the 5 March 1979 event in the subsequent years was a series of recurrent bursts observed in the Konus experiment [32]. In the period 1979-1983, 14 bursts were detected altogether with sufficiently precise localization (Fig.9). Three more bursts from this source were observed from one Venera spacecraft only when the other instrument was turned off. By the general pattern of their time profiles and energy spectra these events did not differ from the other recurrent bursts. However the directional accuracy for them was, accordingly, less precise, the corresponding source positions representing circles of $\approx 15^{\circ}$. Therefore they are not shown in Fig.9.

The persisting activity of GBS0526-66 advocated the

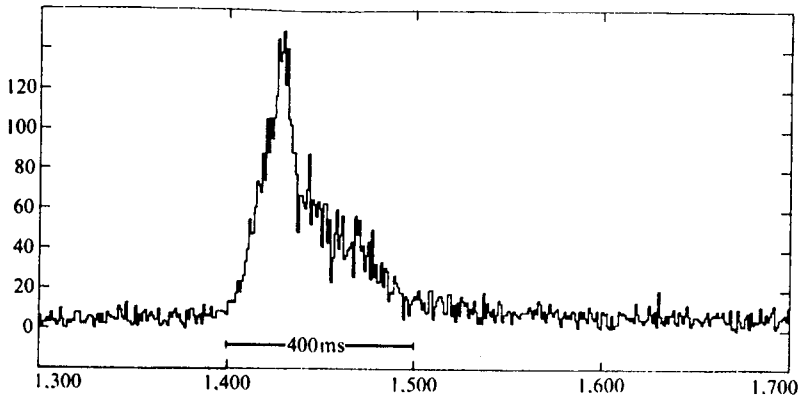


Fig.10. An optical flash presumed to originate in GB 0526-66 [34]

arrangement of optical patrolling of this source at several observatories. Of particular interest were the observations during the time period specified by Rothschild and Lingenfelter [33]. Several optical flashes from this region have been detected [34] (Fig.10). Unfortunately, the Venera 13 and 14 missions were terminated at the time, while simultaneous optical observations from different points failed. However the results of these observations appear promising and plans are under way to continue them.

5. Source Localization. A few cases of fairly precise localization of gamma-ray burst sources on the celestial sphere by triangulation are vastly outnumbered by source position measurements of modest and low accuracy. The bulk of these data were obtained in observations by Venera 11-14.

Fig.11 displays source positions of 160 gamma-ray bursts on the celestial sphere in galactic coordinates. The map does not include bursts localized as annuli-of-position and the cases where two alternative positions were obtained for a source. The sources are distributed over the sky in a random way with no noticeable clustering towards the galactic plane or the galactic center. Note, however, a certain asymmetry between the northern and southern hemispheres [35]. Fig.12 presents the source distribution in galactic latitude vs. the expected isotropic occurrence. 96 sources are found in the northern, and 64 in the southern hemisphere; the mean expected number being 80. The discrepancy is $\sim 2.5\sigma$, however it remains unclear whether it is real or originates from unaccounted for instrumental effects.

The burst distribution in intensity, i.e. in the total energy flux S (erg/cm^2), is usually presented in the $\log N(>S)$ - $\log S$ coordinates. The strong deviation of the experimental distributions from the $-3/2$ law is in a striking disagreement with the isotropic angular distribution obtained if one assumes a constant energy release in the

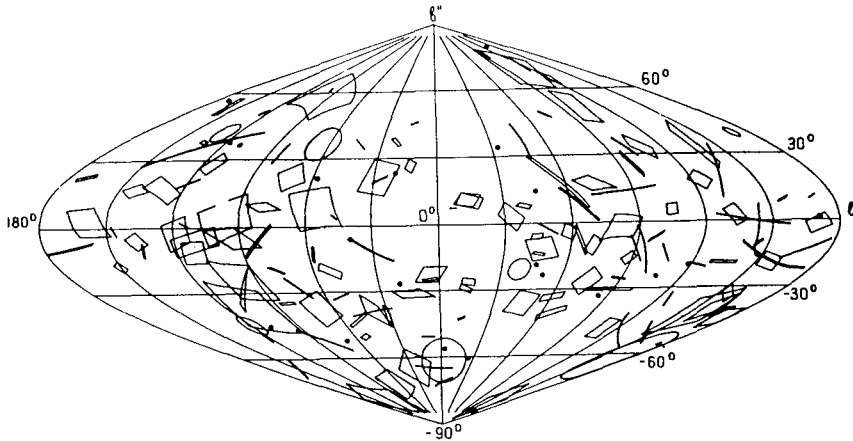


Fig.11. Sky map in galactic coordinates with positions of gamma-ray burst sources

sources. Several attempts were made to estimate the parameters of source spatial distribution from the observed $\log N - \log S$ plots, assuming various luminosity distribution functions (Fig.13) [36,37]. However no reliable estimates of the spatial distribution of sources from the $\log N - \log S$ plot can be obtained. The large extent of the measured values of S ranging from

10^{-7} to 10^{-3} erg/cm^2 does not correspond to the difference in distance scales to the closest and remotest of the observed sources. The spread in the values

of S is determined predominantly by the broad distribution of gamma-ray bursts in duration and large variations between the energy spectra. Burst distributions in peak power P , $\text{erg}/\text{cm}^2 \text{ s}$, $\log N(>P) - \log P$, seem to be more realistic [38].

However this form of the data presentation also distorts the shape of the distribution. Gamma-ray burst detectors are not bolometric devices. In the detection and measurement of a burst they operate with count rates. Therefore the most appropriate form of data presentation is the

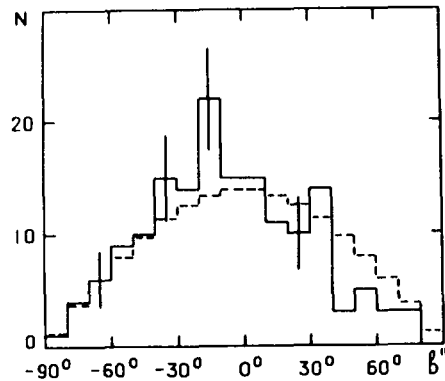


Fig.12. Source distribution in galactic latitude. Dashed line: expected relation for a random spatial distribution of the sources

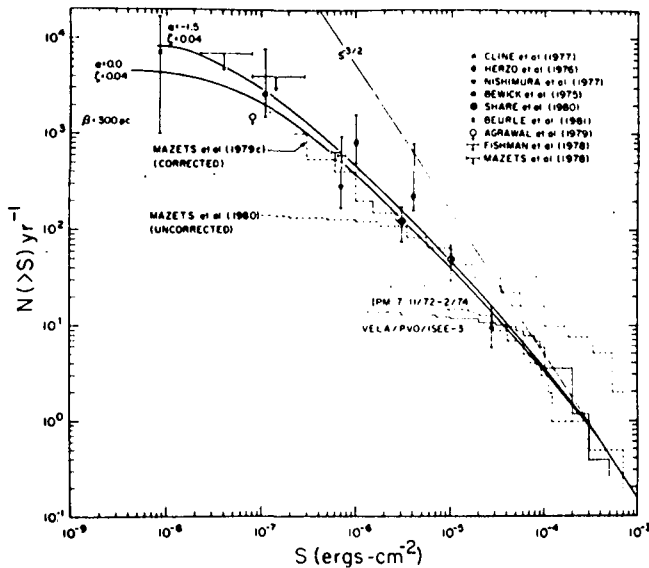


Fig.13. A comparison of some source spatial distribution models with $\log N - \log S$ plots [36]

$-\log n_{\max}$. Since the count rate n_{\max} was determined in $1/4$ s intervals, this data set does not include short bursts. As follows from the graphs, the distribution $\log N - \log n_{\max}$ which is the least subject to distortions shows full agreement with the $-3/2$ law. The deviations in the region of $n_{\max} = 10^2 - 4 \times 10^2$ can undoubtedly be attributed to the loss of weak events near the detection threshold.

The range of n_{\max} covered by observations, $\sim 10^2 - 4 \times 10^3 \text{ s}^{-1}$, is very narrow. It corresponds only to a factor ≈ 6 difference in distances to the closest and the remotest of the observed sources. Thus the $\log N - \log n_{\max}$

plot is in full agreement with an isotropic distribution of the sources over the celestial sphere. This implies that over the region of space corresponding to the sensitivity of the instrumentation used the gamma-ray bursts sources are distributed uniformly. On the basis of these data alone one cannot decide between the galactic and metagalactic models of gamma-ray bursts. Evidence for the gamma-ray bursts being associated with neutron stars attests to the validity of the galactic models. Covering by observations the region of space above the galactic plane where the spatial distribution of the sources may change would apparently require a substantial increase of burst detector sensitivity by ten or

distribution of burst occurrence frequency vs. maximum count rate in the time profile, $\log N - \log n_{\max}$. This

approach has already been discussed as applied to the data of Venera 11 and 12 [39,40]. We have now at our disposal a sufficiently large homogeneous set of observational data from Venera 11-14. In Fig.14 these data are presented in the form of three plots: $\log N(>S) - \log S$, $\log N(>P) - \log P$, and $\log N(>n_{\max})$

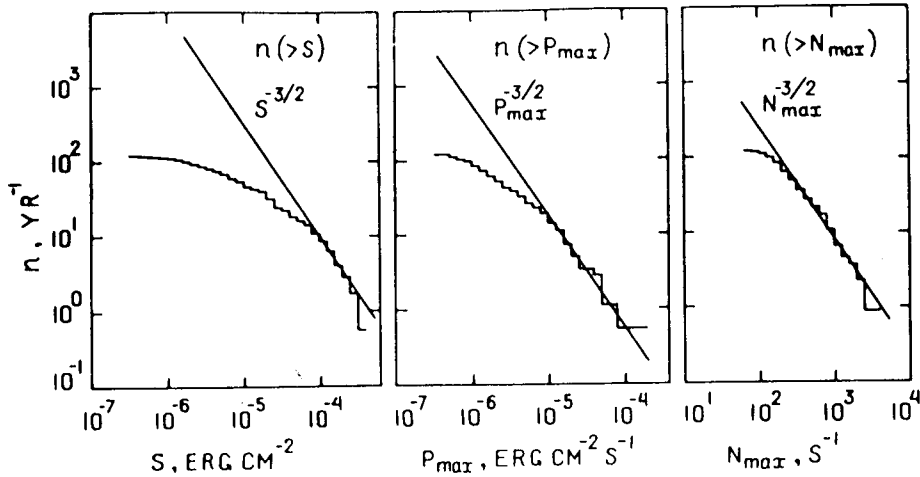


Fig.14. A comparison of three methods of data presentation. Only $\log N(>n_{\max}) - \log n_{\max}$ distribution provides unequivocal interpretation

more times. Estimates of distances to the sources are at present closely connected with the existing physical models of bursts, including the sources of energy and emission mechanism. Thermonuclear models have apparently greater potential for the explanation of the origin of gamma-ray bursts [41-43].

6. Thermonuclear Scenario of a Gamma-Ray Burst. The major characteristics of gamma-ray bursts which should be taken into account in each model are as follows:

(1) By their duration the bursts are divided into two classes, namely, short (< 1 s) and long (1 s to a few minutes) ones.

(2) Long events may exhibit both a simple and very complex time structure.

(3) At least some of long bursts are preceded by weak precursors leading the bursts by 10 - 100 s.

(4) The continuum spectra of bursts evolve rapidly in time. The emission temperature correlates with emission intensity in the time profile.

(5) The burst energy spectra reveal spectral features of two types.

(6) The absorption (most probably cyclotron) features are in most cases the strongest in the initial phase of the burst.

(7) The broad annihilation lines are also the strongest in the beginning of the burst or at intense peaks of the time profile.

(8) The total energy release in a gamma-ray burst is

not constant. It grows approximately proportionately with event duration.

(9) Gamma-ray bursts may be accompanied by intense X-ray emission.

(10) The bursts may apparently be accompanied by optical flashes.

(11) When in quiescent state, the burst sources are so weak that one still has not succeeded in identifying them by emission in the X-ray and optical ranges.

The thermonuclear model of Woosley and Wallace [41] appears to account for these characteristics. It assumes that gamma-ray bursts originate in thermonuclear explosions on accreting, strongly magnetized neutron stars in binaries with a companion star of a late spectral class.

The suggested brief scenario of the burst is related closely to this model. However, observational data make us abandon the simplifying assumption of Woosley and Wallace that the accreting matter accumulates and is confined within a mm^2 , $\sim 10^{-3}$, polar cap region of the surface of the neutron star. The accumulated matter may apparently cover a fraction of the surface ranging from 10^{-3} to 0.1 or even greater. This may be due either to a spreading of the matter during the interval between successive bursts or directly to accretion on such a part of the surface. The distribution of matter over this spot may be extremely inhomogeneous, possibly due to the complex multipolar field structure on the neutron star surface. The thickness of the layer decreases, on the average, as one moves away from the center of the region (Fig.15). The matter in the layer undergoes preburst evolution. Stable burning of hydrogen in pycnonuclear reactions results in accumulation of helium. As soon as the helium layer density in the central part of the spot reaches a critical level, $\sim 10^{20} \text{ g/km}^2$, thermonuclear burning of helium becomes temperature-unstable. Thermonuclear runaway occurs and propagates towards the periphery of the spot.

Estimates of the lateral velocity of deflagration front are uncertain, $\sim 50\text{-}200 \text{ m/s}$ [42]. This velocity apparently is not constant. It depends on density and magnetic

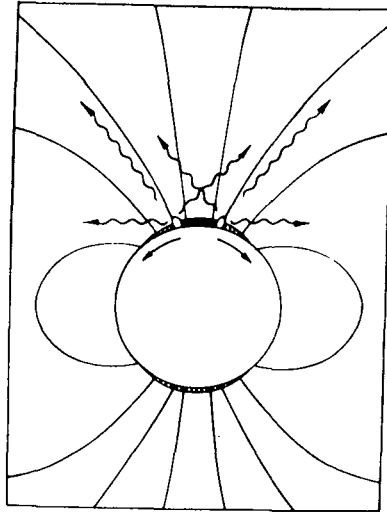


Fig.15. A thermonuclear scenario of cosmic gamma-ray burst

field. The different duration and large-scale time structure of long bursts are connected with propagation of the deflagration front across the region with an inhomogeneous distribution of fuel. The finer details in the time profile reflect apparently the front instabilities.

The energy released at the base of the layer is transported rapidly up to the surface by Alfvén waves and dissipates there [43,44]. Hot plasma with a temperature

$\gtrsim 10^9$ K is confined in the transverse direction by magnetic field while expanding vertically. On the neutron stellar surface a hot annular shell up to a few hundred meters high appears and propagates together with the annular burning region towards the periphery of the layer (Fig.15). The hot plasma pressure distorts drastically the magnetic field at the shell edge. Hence a magnetic field perturbation will propagate together with burning zone. The strong electric fields thus created accelerate electrons up to relativistic energies. Comptonization on fast electrons will produce very many hard photons. However the neutron star's magnetosphere is opaque to photons of energy > 1 MeV due to magnetic pair production (γ, B) [45]. The collisions of hard photons (γ, γ) are likewise accompanied by pair creation [46]. Thus a pair plasma shell will form around the hot cloud of thermonuclear ash. The electrons and positrons lose rapidly their transverse energy by synchrotron emission. Before annihilation they move along magnetic field lines. Acceleration of particles in the radiation field may affect their longitudinal energy distribution such that the annihilation spectrum will acquire a characteristic shape: of a broad line with an extended hard wing (Figs.5 and 6). This radiation can escape from the magnetosphere without appreciable attenuation only in a collimated beam at small angles to the magnetic field. The continuum emission is close to isotropic and reveals a fast falloff of intensity with increasing photon energy (Fig.2).

There is an intriguing possibility that the temperature at the trailing edge of the annular emitting region may be lower, in which case the annihilation emission will be associated predominantly with the leading edge. The cooling matter of the photosphere at the trailing edge will stream down rapidly towards the stellar surface on the free fall time scale. Radiation pressure will drive part of the matter from the photosphere away along the field lines creating a wind. Due to the negative temperature gradient in the photosphere, a cyclotron absorption line may appear in the continuum.

As the burst keeps developing, the annular burning shell passes through a layer with decreasing thickness. The energy released per unit area decreases. This results in a softening of the continuum and a reduction in intensity of the annihilation and cyclotron features.

The X-ray emission is naturally related to the cooling

of thermonuclear ash remaining after the passage of the burning shell.

There is little known about the optical flashes at present. They seem to be connected with a reprocessing of the gamma-ray burst on matter in the vicinity of the neutron star, namely, either in the accreting disc or in the plasma ejected during the burst. The suggested flash recurrence time, $\lesssim 1 \text{ yr}^{-1}$ [47], is difficult to reconcile with the gamma-ray burst observations and the thermonuclear model.

The thermonuclear model permits evaluation of the distance scales to the burst sources. Single-pulse bursts 5-10 s long correspond, within our scenario, to the explosion of a region 1 to 2 km in radius. According to model I of Woosley and Wallace [41] the energy released in gamma rays in such a burst should be $\sim 5 \times 10^{38}$ erg. The brightest events of this type observed thus far have a total fluence $S \sim 2 \times 10^{-5}$ erg/cm². This leads to an estimate of distance to the nearest sources of ≈ 300 pc. Then, in accordance with the relation $\log N - \log n_{\text{max}}$, the farthest of the detected burst sources could be at a distance of ≈ 1.8 kpc.

For the burst recurrence time $\gtrsim 10$ yr the average accretion rate should be $\lesssim 4 \times 10^{-14} M_{\odot} / \text{yr}$, and the constant X-ray luminosity of the source $\sim 5 \times 10^{32}$ erg/s. These estimates support the assumption of the neutron star's companion in the binary being a star of the latest spectral class with low mass and luminosity. The possibility of explaining short bursts as due to detonation thermonuclear explosions by model II [41] appears very attractive. In this case, however, the corresponding distance estimates will increase ten times. Still, detonation models involving smaller energy release can apparently be also designed.

Thus the thermonuclear model developed for gamma-ray bursts appears to conform to the major observational characteristics of bursts.

The most serious difficulty for this model may come from the observation of a weak feature in the burst time profile, namely, of the precursors. These weak pulses are definitely connected with the main phase of the burst and do not exist independently of it. Otherwise one would have observed numerous weak recurrent bursts from the same source. It is difficult to account for the situation when the process of thermonuclear burning, once initiated, dropped drastically in intensity, only to flare up again a few tens of seconds later.

7. Conclusion. Cosmic gamma-ray bursts remain one of the most intriguing and complex problems in astrophysics. There is much work ahead, both experimental and theoretical.

before we may hope to come closer to the understanding of the nature of this mysterious phenomenon.

References

1. Klebesadel, R.W. et al., (1973), *Astrophys. J.* 182, L85.
2. Mazets, E.P., and Golenetskii, S.V., (1981), *Astrophys. Space Sci.* 75, 47.
3. Klebesadel, R.W. et al., (1982), in *Gamma-Ray Transients and Related Astrophysical Phenomena*, eds. R.E.Lingenfelter, H.S.Hudson & D.M.Worrall, AIP Conf. Proc. No 77, NY, p.1.
4. Mazets, E.P. et al., (1982), *Astrophys. Space Sci.* 84, 173.
5. Hurley, K., (1984), in *High Energy Transients in Astrophysics*, ed.S.E.Woosley, AIP Conf. Proc. No 115, NY, p.363.
6. Norris, J.P. et al., (1984), *ibid.*, p.367.
7. Pizzichini, G., (1981), *Astrophys. Space Sci.* 75, 205.
8. Wood, K.S., (1984), in *High Energy Transients in Astrophysics*, ed. S.E.Woosley, AIP Conf. Proc. No 115, NY, p.409.
9. Desai, U.D., (1981), *Astrophys. Space Sci.* 75, 15.
10. Knight, F.K. et al., (1981), *Astrophys. Space Sci.* 75, 21.
11. Mazets, E.P. et al., (1982), *Astrophys. Space Sci.* 82, 261.
12. Ramaty, R. et al., (1981), *Astrophys. Space Sci.* 75, 193.
13. Liang, E.P., (1981), *Nature* 299, 378.
14. Teegarden, B.J., (1984), in *High Energy Transients in Astrophysics*, ed.S.E.Woosley, AIP Conf. Proc. No 115, NY, p. 352.
15. Katz, J.I., (1982), *Astrophys. J.* 260, 371.
16. Lamb, D.Q., (1984), *Ann. NY Acad. Sci.* 422, 237.
17. Colgate, S.A. et al., (1984), in *High Energy Transients in Astrophysics*, ed. S.E.Woosley, AIP Conf. Proc. No 115, NY, p.548.
18. Mazets, E.P. et al., (1981), *Nature* 290, 378.
19. Golenetskii, S.V. et al., (1983), *Nature* 306, 451.
20. Barat, C. et al., (1984), *Astrophys. J.* 286, L11.
21. Share, G.H. et al., (1982), in *Gamma-Ray Transients and Related Astrophysical Phenomena*, eds. R.E.Lingenfelter, H.S.Hudson & D.M.Worrall, AIP Conf. Proc. No 77, NY, p.45.
22. Nolan, P.L. et al., (1984), in *High Energy Transients in Astrophysics*, ed. S.E.Woosley, AIP Conf. Proc. No 115, NY, p.399.
23. Aptekar, R.L. et al., (1985), these Proceedings, 001.1-3.
24. Ramaty, R., and Mészáros, P., (1981), *Astrophys. J.* 250, 384.
25. Aharonyan, F.A. et al., (1983), *Astrophys. Space Sci.* 93, 229.
26. Hueter, G.J., (1984), in *High Energy Transients in Ast-*

- rophysics, ed. S.E.Woosley, AIP Conf. Proc. No 115, NY, p.373.
27. Laros, J.G. et al., (1984), *Astrophys. J.* 286, 681.
 28. Hurley, K., (1982), in *Gamma-Ray Transients and Related Astrophysical Phenomena*, eds. R.E.Lingenfelter, H.S.Hudson & D.M.Worrall, AIP Conf. Proc. No 77, NY, p.85.
 29. Cline, T.L. et al., (1984), *Astrophys. J.* 286, L15.
 30. Schaefer, B.E., (1981), *Nature* 294, 722.
 31. Schaefer, B.E. et al., (1984), *Astrophys. J.* 286, L1.
 32. Golenotskii, S.V. et al., (1984), *Nature* 307, 41.
 33. Rothschild, R.E., and Lingenfelter, R.E., (1984), *Nature* 312, 737.
 34. Pedersen, H. et al., (1984), *Nature* 312, 46.
 35. Vedrenne, G., (1981), *Phil. Trans. Roy. Soc.* A301, 645.
 36. Jennings, M.C., (1982), *Astrophys. J.* 258, 110.
 37. Jennings, M.C., (1984), in *High Energy Transients in Astrophysics*, ed. S.E.Woosley, AIP Conf. Proc. No 115, NY, p.412.
 38. Mazets, E.P. et al., (1980), *Pis'ma v Astron. Zhurnal* 6, 609.
 39. Belli, B.M., (1984), in *High Energy Transients in Astrophysics*, ed. S.E.Woosley, AIP Conf. Proc. No 115, NY, p.426.
 40. Lund, N., (1985), private communication.
 41. Woosley, S.E., and Wallace, R.K., (1982), *Astrophys. J.* 258, 716.
 42. Woosley, S.E., (1984), in *High Energy Transients in Astrophysics*, ed. S.E.Woosley, AIP Conf. Proc. No 115, NY, p.485.
 43. Bonazzola, S. et al., (1984), *Astron. Astrophys.* 136, 89.
 44. Mitrofanov, I.G., and Ostryakov, V.M., (1981), *Astrophys. Space Sci.* 77, 469.
 45. Daugherty, J.K., and Harding, A.K., (1983), in *Positron-Electron Pairs in Astrophysics*, eds. M.L.Burns, A.K.Harding & R.Ramaty, AIP Conf. Proc. No 101, NY, p.387.
 46. Burns, M.L., and Harding, A.K., (1983), *ibid.*, p.416.
 47. Schaefer, B.E., and Cline, T.L., (1985), *Astrophys. J.* 289, 490.